J|A|C|S
COMMUNICATIONS

Published on Web 11/02/2006

# Effect of Surface Functionalization of MCM-41-Type Mesoporous Silica Nanoparticles on the Endocytosis by Human Cancer Cells

Igor Slowing, Brian G. Trewyn, and Victor S.-Y. Lin*

*Department of Chemistry, Iowa State University, Ames, Iowa 50011-3111*

Received June 28, 2006; Revised Manuscript Received September 28, 2006; E-mail: vsylin@iastate.edu

Recent studies on the interaction between surface-functionalized inorganic nanoparticles and animal cells have shown great potential for utilizing these size-defined nanomaterials for various biomedical and biotechnological applications, such as cell type recognition, disease diagnosis, intracellular imaging, and drug/gene delivery. In particular, several recent reports,[1−5] including our own studies, have shown that mesoporous silica nanoparticles can be efficiently endocytosed by mammalian cells. The large surface areas and pore volumes of these materials offer the possibility of encapsulating and delivering large quantities of biogenic molecules through different cell membranes and to various intracellular targets. Furthermore, it has been demonstrated recently that the mesopores of these nanoparticles can be closed and opened at will by various capping/release strategies.[1,3,6] These new breakthroughs make the surface-functionalized MSNs excellent candidates for intracellular controlled-release delivery. To realize this goal, an important prerequisite would be to understand the mechanism of cellular uptake of these surface-functionalized mesoporous silica nanoparticles, so that the uptake of MSNs by different cell types can be regulated. For example, to use these MSNs as efficient intracellular delivery vehicles it would be important to use different surface functional groups to manipulate the rate of escape of MSNs from endosomes to cytosol and other intracellular organelles. To the best of our knowledge, no report has examined the effect of surface functional groups on the cellular uptake properties of these mesoporous silica-based nanoparticles. Herein, we report on the synthesis of a series of organically functionalized MSNs and investigate the mechanism and efficiency of endocytosis of these materials with different charge profiles on human cervical cancer cells (HeLa).

First, we synthesized a fluorescein-functionalized, MCM-41-type mesoporous silica nanoparticle material (FITC-MSN).[7] As shown in Figure 1, FITC-MSN has an average particle diameter of 150 nm. The MCM-41-type mesoporous structure with a 2.4 nm average pore diameter and a surface area of 850 $m^2/g$ was confirmed by powder X-ray diffraction (XRD), nitrogen sorption isotherms, and scanning and transmission electron microscopy (SEM and TEM, respectively) measurements.[7] Three functional groups, 3-aminopropyl (AP), *N*-(2-aminoethyl)-3-aminopropyl (AEAP), and *N*-folate-3-aminopropyl (FAP), were grafted onto the external surface of the FITC-MSN by refluxing 6 mmol of the corresponding trimethoxysilyl derivatives with 1 g of FITC-MSN in toluene for 20 h. The amino groups of the 3-aminopropyl and the *N*-(2-aminoethyl)-3-aminopropyl were transformed into guanidinopropyl (GP) and 3-[*N*-(2-guanidinoethyl)guanidino]propyl (GEGP) groups, respectively, via a literature procedure.[8] The amount of surface-anchored AP, GP, GEGP, and FAP groups were determined by solid-state direct polarization $^{29}Si$ NMR to be 1.5, 1.3, 0.97, and 0.89 mmol/g, respectively. After the grafting of these groups, the surfactant template (CTAB) molecules were removed from the MSNs by refluxing 1.0 g of the materials in 100 mL of methanol and 1 mL of concentrated HCl.

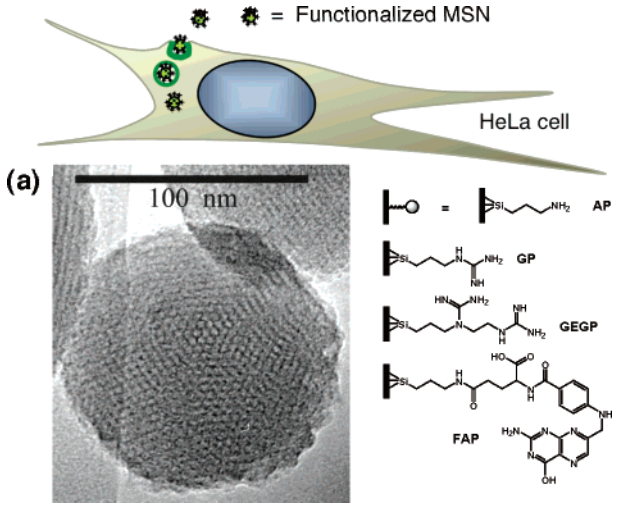


***Figure 1.*** Schematic representation of the endocytosis of organically functionalized mesoporous silica nanoparticles (MSNs) by a human cervical cancer cell (HeLa). **(a)** TEM image of a fluorescein-functionalized MSN (FITC-MSN).

***Table 1.*** ζ-Potentials and $ED_{50}$ for Cellular Uptake of the MSNs

| material | ζ-potential [mV] | $ED_{50}$ (μg/mL) |
|---|---|---|
| FITC−MSN | −34.73 ± 3.50 | 12.35 |
| AP-MSN | −4.68 ± 1.54 | 10.95 |
| GP-MSN | −3.25 ± 0.275 | 8.8 |
| GEGP-MSN | +0.57 ± 0.095 | 6.39 |
| FAP-MSN | +12.81 ± 1.60 | 2.73 |

In contrast to the zeta potential (ζ-potential) of −34.73 mV for FITC-MSN, the values of ζ-potential for AP-, GP-, GEGP-, and FAP-functionalized FITC-MSNs in 100 mM PBS buffer (pH 7.4) increased positively from −4.68 to +12.81 mV, respectively, as outlined in Table 1.

To examine the biocompatibility of MSNs, we compared the cell growth profiles of HeLa cultures with and without MSNs (0.1 mg/mL) for 4 days. Our results showed no difference in growth with or without the MSNs.[7]

To investigate the uptake of these organically functionalized MSNs, different concentrations of MSNs were introduced to HeLa cell cultures seeded at $1.0 \times 10^5$ cells/mL for 10 h in serum-free media. The degree of endocytosis was determined by quantifying live cells that exhibited green fluorescence with flow cytometry. To ensure the fluorescence observed in the flow cytometry measurements was indeed from the MSNs that have been endocytosed, a fluorescence quencher, Trypan Blue, was included in the cell suspension. Since Trypan Blue cannot penetrate the membranes of living cells, it could only quench the fluorescence of those MSNs that are adsorbed on the exterior surface of cells.[9] The plots of the logarithms of the concentrations of MSNs versus the percentages of cells that took up the MSNs showed a sigmoidal behavior, which


10.1021/ja0645943 CCC: $33.50 

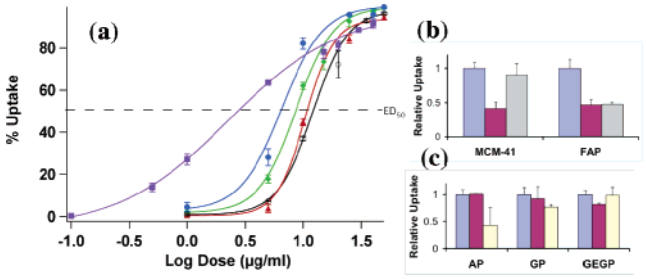


***Figure 2.*** (a) Uptake of the synthesized MSNs as a function of their concentration: (○) FITC-, (▲) AP-, (◆) GP-, (●) GEGP-, and (■) FAP-MSNs. **(**b**)** and **(**c**)** Uptake of the materials in absence (blue bars) and presence of a series of inhibitors: 450 mM sucrose (prune); 1 mM folic acid (gray); 200 mM genistein (cream).

is typical of dose−response endocytosis (Figure 2a). The degrees of uptake of these MSNs were determined by their $ED_{50}$ values.

The uptake of nonfunctionalized, negatively charged silica materials by cells has been found to occur through a nonspecific adsorptive endocytosis,[5] and the resting potentials of cell membranes are normally negative (−50 mV for HeLa).[10] The relationship between the $ED_{50}$ values and the ζ-potentials of these surface-functionalized MSNs is summarized in Table 1. Flow cytometry results suggested that the endocytosis of MSN could be manipulated by different surface functionalization. In addition to the surface charge effect, it is well-known that the membranes of human cancer cells are abundant with folate receptors.[11] The folate groups on FAP-MSN could also play an active role in facilitating a receptor-mediated endocytosis.

To investigate the possible mechanism of endocytosis of the different MSNs, we tested the cellular uptake of these materials in presence of specific inhibitors. Our results indicated that only the FITC- and FAP-MSNs are endocytosed via a clathrin-pitted mechanism, as the uptakes were inhibited by 450 mM sucrose (Figure 2b,c). In addition, the uptake of FAP-MSN was partially inhibited in presence of 1 mM folic acid, whereas the endocytosis of FITC-MSN was not perturbed (Figure 2b). This observation along with the higher uptake observed for FAP-MSN suggests that the mechanism of endocytosis for this material is mediated by folic acid receptors on the HeLa cell surface. In contrast, the endocytosis of AP- and GP-MSNs was affected by a caveolar inhibitor, genistein (Figure 2c), suggesting that these materials are endocytosed via a caveolae-mediated mechanism. The uptake mechanism of GEGP remains unclear because the endocytosis was not dramatically affected by any of the inhibitors.

To study the impact of surface functionality in endosome escape, we stained the endosomes with a red fluorescent endosome marker (FM 4-64) and monitored the confocal fluorescence micrographs (Figure 3)[7] of FITC-MSNs with different functional groups in HeLa cells. The green fluorescent spots in Figure 3a represent the FITC-MSNs that were able to escape the endosomes, whereas those that were trapped inside the vesicles are yellow in color, which is the result of overlapping red (endosome) and green (MSN) spots. We found that the more negatively charged FITC- and AP-MSNs appeared to be able to escape from endosomes within 6 h, while those with more positive ζ-potentials, such as GP-, GEGP- and FAP-MSNs, remained trapped within endosomes.[7] This behavior

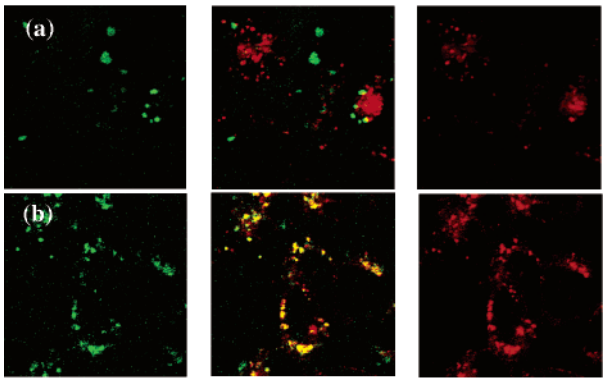


***Figure 3.*** Confocal fluorescence images of HeLa cells stained with FM 4-64 and 40 μg/mL suspensions of **(**a**)** FITC-MSN and **(**b**)** FAP-MSN after 6 h of introduction. The fluorescent images (left) show the MSNs (green) and FM 4-64-labeled endosomes (red). The corresponding phase contrast images are displayed on the right.

could be attributed to the Proton Sponge effect,[12] where the more negatively charged materials would have a better buffering capacity, which is important for the endosome escape.[12]

In conclusion, we have demonstrated the uptake of MCM-41-type mesoporous silica nanoparticles by HeLa cells can be regulated by different surface functionalization. Our results indicated that these surface functionalities could also affect MSN's ability to escape endosomal entrapment, which is a key factor in designing effective intracellular delivery vehicles.

**Acknowledgment.** This research was supported by the NSF (CHE-0239570). We thank the cell and hybridoma facility of ISU for their assistance.

**Supporting Information Available:** Syntheses and characterizations of MSNs, cell cultures, flow cytometry, confocal fluorescence microscopy, and immunochemistry experiments. This material is available free of charge via the Internet at http://pubs.acs.org.

## References

(1) Giri, S.; Trewyn, B. G.; Stellmaker, M. P.; Lin, V. S. Y. *Angew. Chem., Int. Ed.* **2005**, *44*, 5038−5044.
(2) Huang, D.-M.; Hung, Y.; Ko, B.-S.; Hsu, S.-C.; Chen, W.-H.; Chien, C.-L.; Tsai, C.-P.; Kuo, C.-T.; Kang, J.-C.; Yang, C.-S.; Mou, C.-Y.; Chen, Y.-C. *FASEB J.* **2005**, *19*, 2014−2016.
(3) Lai, C.-Y.; Trewyn, B. G.; Jeftinija, D. M.; Jeftinija, K.; Xu, S.; Jeftinija, S.; Lin, V. S. Y. *J. Am. Chem. Soc.* **2003**, *125*, 4451−4459.
(4) Lin, Y.-S.; Tsai, C.-P.; Huang, H.-Y.; Kuo, C.-T.; Hung, Y.; Huang, D.-M.; Chen, Y.-C.; Mou, C.-Y. *Chem. Mater.* **2005**, *17*, 4570−4573.
(5) Xing, X.; He, X.; Peng, J.; Wang, K.; Tan, W. *J. Nanosci. Nanotechnol.* **2005**, *5*, 1688−1693.
(6) Gruenhagen, J. A.; Lai, C.-Y.; Radu, D. R.; Lin, V. S. Y.; Yeung, E. S. *Appl. Spectrosc.* **2005**, *59*, 424−431.
(7) See Supporting Information.
(8) Bernatowicz, M. S.; Youling, W.; Matsueda, G. R. *J. Org. Chem.* **1992**, *57*, 2497−2502.
(9) Hed, J.; Hallden, G.; Johansson, S. G.; Larsson, P. *J. Immunol. Methods* **1987**, *101*, 119−125.
(10) Szabo, I.; Brutsche, S.; Tombola, F.; Moschioni, M.; Satin, B.; Telford, J. L.; Rappuoli, R.; Montecucco, C.; Papini, E.; Zoratti, M. *EMBO J.* **1999**, *18*, 5517−5527.
(11) Ladino, C. A.; Chari, R. V. J.; Bourret, L. A.; Kedersha, N. L.; Goldmacher, V. S. *Int. J. Cancer* **1997**, *73*, 859−864.
(12) Boussif, O.; Lezoualc'h, F.; Zanta, M. A.; Mergny, M. D.; Scherman, D.; Demeneix, B.; Behr, J.-P. *Proc. Natl. Acad. Sci. U.S.A.* **1995**, *92*, 7297−7301.

JA0645943